amines in (amine)iron(III) complexes, yielding imine- or di-imine-iron(II) complexes.

The oxidation of $[FeL_2]^{2+}$ with a variety of pulse radiolytically generated radicals produced $[FeL_2]^{3+}$, and at pH >10 the $[FeL(L\text{-}H)]^{2+}$ species at nearly diffusion controlled rates. Laser photolysis (λ = 248 nm) of $[FeL_2]^{2+}$ at pH 8-13 produced in a monophotonic process the hydrated electron and $[FeL_2]^{3+}$ (or its deprotonated form).

Finally it was shown that $[FeL(L\text{-}H)]^{2+}$ reduces the ascorbate dianion, yielding $[FeL_2]^{2+}$ and the ascorbate radical anion. From equilibrium kinetics of this reaction it has been possible to confirm a previous determination of the redox potential of the $AS^{-/2-}$ couple.

Acknowledgment. We are grateful to the Fonds der Chemischen Industrie for financial support of this work.

Registry No. $[FeL_2](ClO_4)_2$, 111958-64-6; $[FeL_2](ClO_4)_3$, 111958-66-8; $[FeL(L\text{-}H)]^{2+}$, 111958-67-9; $I_2^{\bullet-}$, 12190-71-5; $(SCN)_2^{\bullet-}$, 34504-17-1; $Br_2^{\bullet-}$, 12595-70-9; $OH^{\bullet}$, 3352-57-6; $PhO^{\bullet}$, 2122-46-5; H_2O_2, 7722-84-1; O_2, 7782-44-7; ascorbate(1-), 299-36-5; ascorbate(2-), 63983-50-6; 1,4,7-triazacyclononane, 4730-54-5.

Contribution from the Department of Chemistry, Faculty of Science, Kyushu University 33, Hakozaki, Fukuoka, 812 Japan, and Coordination Chemistry Laboratories, Institute for Molecular Science, Myodaiji, Okazaki, 444 Japan

An Important Factor Determining the Significant Difference in Antiferromagnetic Interactions between Two Homologous (μ-Alkoxo)(μ-pyrazolato-N,N')dicopper(II) Complexes[1]

Yuzo Nishida[2a] and Sigeo Kida*[2b]

Received February 2, 1987

The crystal structures of $Cu_2(L^1)(prz)$ (**1**) and $Cu_2(L^2)(pyz)$ (**2**) were determined by X-ray analysis, where prz denotes a deprotonated anion of pyrazole and HL^1 and HL^2 represent binucleating ligands formed by the condensation of salicylaldehyde with 1,3-diamino-2-propanol and 1,5-diamino-3-pentanol, respectively. Both compounds consist of discrete binuclear units, in which copper atoms are linked by the alkoxide oxygen of the ligand and the pyrazolate nitrogens. Magnetic susceptibility measurements revealed that antiferromagnetic interaction is operating in both compounds. However, the interaction of **2** ($-2J$ = 595 cm^{-1}) is much stronger than that of **1** ($-2J$ = 310 cm^{-1}), irrespective of the small difference in the bridging structure. It is difficult to explain this fact in terms of structural factors on the basis of the so far widely accepted criterions. Instead, the change in the interaction between the magnetic d orbitals and the HOMOs of the pyrazolate nitrogens induced by changes in the size of the chelating rings was estimated for the energy and overlap of these orbitals. It was concluded that the pyrazolate bridge contributes little to the antiferromagnetism of **2**, but in the case of **1**, the pyrazolate bridge operates countercomplementarily toward the antiferromagnetism effected by the alkoxide bridge, bringing about the weaker antiferromagnetism for **1**.

Introduction

Magnetisms of bis(μ-hydroxo)- or bis(μ-alkoxo)dicopper(II) complexes have been the subjects of extensive investigations for the last two decades.[3] According to Hatfield and Hodgson, antiferromagnetic interaction between copper(II) ions becomes larger with increasing Cu-O-Cu angle in these complexes.[3,4] This was reasonably explained in terms of quantum-mechanical treatments by Hoffmann et al.,[5] Bencini and Gatteschi,[6] Kahn,[7] and Astheimer and Haase.[8] However, this rule had been confined to doubly bridged systems with the Cu-O-Cu angle in the range 95-105° until McKee et al.[9] and the present authors[10] reported the syntheses and magnetism of copper(II) complexes with a single alkoxide bridge derived from 1,3-diamino-2-propanol, such as **3** (Figure 1). Since in such complexes the Cu-O-Cu angle is much larger (120-135°) than that of the doubly bridged complexes, substantially stronger antiferromagnetic interaction would be expected in spite of the fact that the superexchange paths occur through half of the doubly bridged complexes. In fact, this was found to be true; e.g., $2J = -635$ cm^{-1} for **3**.[10] It was revealed that when another bridging group, such as acetate[10] or azide (end to end),[11] is added to this system, the antiferromagnetic interaction is substantially weakened or enhanced, depending on the second ligand. This fact was reasonably interpreted in terms of Hoffmann's theory that the matching of symmetries of HOMOs of the bridging groups determines whether the two bridges work complementarily or countercomplementarily in the superexchange interaction.[10] This theory is essentially important when the magnetism of a binuclear complex possessing two different bridging groups is considered. This fact has been recognized in some other examples.[11,12]

Recently, Mazurek et al. reported the preparation of dicopper(II) complexes $Cu_2(L^1)(prz)\cdot H_2O$ (**1**·H_2O) and $Cu_2(L^2)(prz)$ (**2**), where H_3L^1 and H_3L^2 are Schiff bases derived from salicylaldehyde and 1,3-diamino-2-propanol or 1,5-diamino-3-pentanol (Figure 2).[13] They determined the crystal structure of

(1) Partly presented at the 25th International Symposium on Coordination Chemistry in Nangjing, China, Aug 1987; see Abstracts, p 105.
(2) (a) Kyushu University. Present address: Department of Chemistry, Faculty of Science, Yamagata University, Koshirakawamachi, Yamagata, 990 Japan. (b) Institute for Molecular Science.
(3) Crawford, U. H.; Richardson, H. W.; Wasson, J. R.; Hodgson, D. J.; Hatfield, W. E. *Inorg. Chem.* **1976**, *15*, 2107.
(4) (a) Hatfield, W. E. *ACS Symp. Ser.* **1974**, *No. 5*, 108. (b) Hodgson, D. J. *Prog. Inorg. Chem.* **1975**, *19*, 173.
(5) Hay, P. J.; Thibeault, J. C.; Hoffmann, R. *J. Am. Chem. Soc.* **1975**, *97*, 4887.
(6) Bencini, A.; Gatteschi, D. *Inorg. Chim. Acta* **1978**, *31*, 11.
(7) Kahn, O. *Inorg. Chim. Acta* **1982**, *62*, 3.
(8) Astheimer, H.; Haase, W. *J. Chem. Phys.* **1986**, *85*, 1427.
(9) (a) McKee, V.; Smith, J. *J. Chem. Soc., Chem. Commun.* **1983**, 1465. (b) Drew, M. G. B.; Nelson, J.; Esho, F. S.; McKee, V.; Nelson, S. M. *J. Chem. Soc., Dalton Trans.* **1982**, 1837.
(10) (a) Nishida, Y.; Takeuchi, M.; Takahashi, K.; Kida, S. *Chem. Lett.* **1985**, 631. (b) Nishida, Y.; Kida, S. *J. Chem. Soc., Dalton Trans.* **1986**, 2633.
(11) (a) McKee, V.; Zvagulis, M.; Reed, C. A. *Inorg. Chem.* **1985**, *24*, 2914. (b) McKee, V.; Dagdigian, J. V.; Bau, R.; Reed, C. A. *J. Am. Chem. Soc.* **1981**, *103*, 7000.
(12) Mallah, T.; Baillot, M.-L.; Kahn, O.; Gouteron, J.; Jeannin, S.; Jeannin, Y. *Inorg. Chem.* **1986**, *25*, 3058.

0020-1669/88/1327-0447$01.50/0

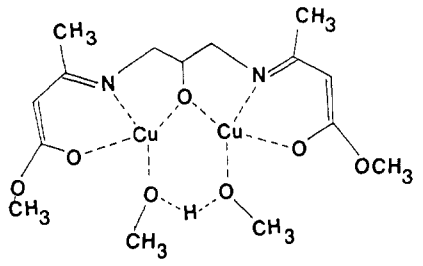

Figure 1. Complex **3**.

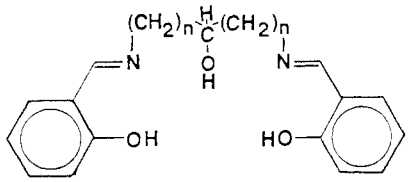

Figure 2. Binucleating ligands HL^1 (n = 1) and HL^2 (n = 2).

1·H_2O by X-ray analysis showing that the two copper ions are bridged by an alkoxide oxygen and by the N_2 moiety of the pyrazolate ligand. Antiferromagnetic interactions were observed for both complexes, the $-2J$ value (the energy separation between the spin-triplet and spin-singlet states) being evaluated as 240 and >1000 cm^{-1} for **1**·H_2O and **2**, respectively.

Because of the large difference in $-2J$ values for those complexes, we have determined the crystal structure of **2** in order to clarify the origin of the difference in magnetic interactions of these homologous compounds. The result has revealed that there is no essential difference in molecular structure between **2** and **1**·H_2O. We have also carried out magnetic susceptibility measurements for **2** over the temperature range 300–80 K and obtained a different $-2J$ value of 595 cm^{-1}. The reason for such a discrepancy is not clear; the compound might have two different crystal modifications. In the course of reexamination of the magnetism of the L^1 complex, we have obtained crystals of $Cu_2(L^1)(prz)$ (**1**) instead of **1**·H_2O; hence, this compound has also been subjected to X-ray crystal analysis. The result has shown that the structure is quite similar to that of **1**·H_2O, though there is some difference in the $-2J$ values, i.e., 310 cm^{-1} (**1**) and 240 cm^{-1} (**1**·H_2O). Here, it should be noted that there is a significant difference in antiferromagnetic interaction between **1** (or **1**·H_2O) and **2**, in spite of the small difference in the coordination and bridging configuration. It seems difficult to give a reasonable explanation for this fact in terms of the so far widely accepted criterions such as bond angle of the Cu–O–Cu bridge,[3,4] planarity of bonds around the bridging oxygen, or dihedral angle between the two coordination planes.[13] Thus, in this study, we have invoked the complementarity of the orbitals of two bridging groups in order to elucidate the superexchange interaction in these systems.

Experimental Section

Preparation of Compounds. Compound 1. Purple powder was obtained from a mixture of H_3L^1 (2.95 g, 0.01 mol), pyrazole (0.7 g, 0.01 mol), copper(II) acetate monohydrate (4.0 g, 0.02 mol), and triethylamine (4.1 g, 0.04 mol) in methanol. The crude crystals were recrystallized from dimethylformamide. Yield: 3 g. Anal. Calcd for $C_{20}H_{18}N_4Cu_2O_3$: C, 49.08; H, 3.71; N, 11.75. Found: C, 49.14; H, 3.68; N, 11.49.

Compound 2. The crystals were prepared by the method of Mazurek et al.[13] Green needle crystals were obtained by recrystallization from chloroform–ethanol (1:1) solution. Yield: 2 g. Anal. Calcd for $C_{22}H_{22}N_4Cu_2O_3$: C, 51.06; H, 4.28; N, 10.83. Found: C, 51.06; H, 4.24; N, 10.86.

Magnetic Measurements. Magnetic susceptibilities were measured by the Faraday method over the temperature range 80–300 K. The J values were determined by simulating the experimental χ–T curve with the Bleaney–Bowers equation.[14]

Table I. Crystal Data for **1** and **2**

compd	**1**	**2**
space group	monoclinic $P2_1/c$	monoclinic $P2_1/a$
a/Å	12.579 (3)	19.279 (5)
b/Å	13.970 (3)	9.021 (2)
c/Å	11.097 (2)	11.945 (3)
β/deg	104.52 (2)	98.83 (2)
V/Å^3	1887.8 (7)	2052.9 (9)
Z	4	4
F(000)	992	1056
μ(Mo Kα)/cm^{-1}	23.7	21.8
d_{calcd}/g cm^{-3}	1.72	1.67
cryst dimens/mm^3	0.2 × 0.3 × 0.3	0.1 × 0.4 × 0.03
no. of reflcns ($>3\sigma(F_o)$)	3218	2794
R ($=\sum\|\|F_o\| - \|F_c\|\|/\sum\|F_o\|$)	0.048	0.072
R_w [$=(\sum w\|\|F_o\| - \|F_c\|\|^2/\sum w\|F_o\|^2)^{1/2}$] ($w = 1/\sigma(F_o)$)	0.051	0.089

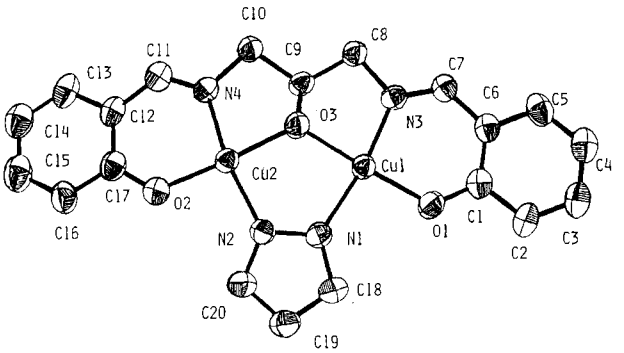

Figure 3. Structure and numbering system for **1**, showing 50% probability thermal ellipsoids.

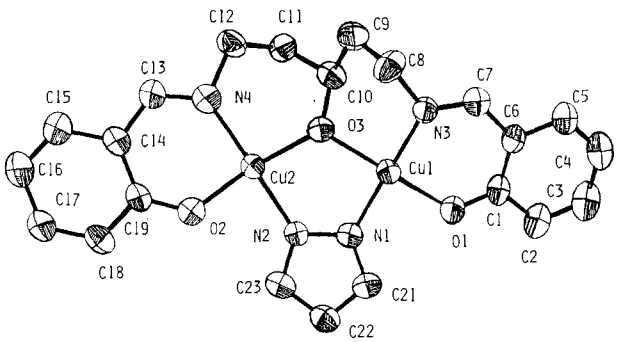

Figure 4. Structure and numbering system for **2**, showing 50° probability thermal ellipsoids.

Crystal Data of Compounds. Dark violet prisms of **1** were obtained by slow crystallization from warm dimethylformamide solution. Green needles of **2** were obtained by slow evaporation of chloroform–ethanol solution. Crystals were mounted on a Rigaku AFC-5 automatic diffractometer with graphite-monochromated Mo Kα radiation (λ = 0.710 69 Å). Automatic centering and least-squares routines were carried out on 25 reflections ($18° < 2\theta < 28°$) to obtain the cell constants. The crystal data are listed in Table I, together with the R and R_w values.

Data Collection. The ω–2θ scan technique was employed to record the intensities for a unique set of reflections for which $3° < 2\theta < 55°$. Three check reflections were measured every 100 reflections: they exhibited no significant decay during the data collection. Intensities were corrected for Lorentz and polarization effects.

Solution and Refinement of the Structure. The positions of Cu atoms were determined by direct methods.[15] Subsequent Fourier syntheses revealed the positions of the remaining non-hydrogen atoms. The structures were refined by a block-diagonal least-squares method with anisotropic thermal parameters used for the non-hydrogen atoms. The final R values are listed in Table I. All scattering factors were taken from ref 16. All calculations were performed on a Facom M-200 computer

(13) Mazurek, W.; Kennedy, B. J.; Murray, K. S.; O'Connor, M. J.; Rodgers, J. R.; Snow, M. R.; Wedd, A. G.; Zwack, P. R. *Inorg. Chem.* **1985**, *24*, 3258.
(14) Bleaney, B.; Bowers, K. D. *Proc. R. Soc. London, A* **1952**, *214*, 451.
(15) Main, P.; Woolfsen, M. M.; Germain, G. "Computer Program for the Automatic Solution of Crystal Structure"; Universities of York, England, and Louvain, Belgium, 1971.

Table II. Atomic Parameters for Compound **1**

atom	x/a	y/b	z/c
Cu1	−0.0052 (1)	0.5921 (0.3)	0.1125 (1)
Cu2	0.1809 (1)	0.6053 (0.3)	−0.0563 (1)
O1	−0.0489 (3)	0.5806 (3)	0.2630 (3)
O2	0.3238 (3)	0.5981 (3)	−0.0770 (4)
O3	0.0314 (3)	0.5990 (3)	−0.0450 (3)
N1	0.1514 (4)	0.5835 (3)	0.1931 (4)
N2	0.2269 (3)	0.5829 (3)	0.1224 (4)
N3	−0.1480 (4)	0.6343 (3)	0.0140 (4)
N4	0.1130 (4)	0.6506 (3)	−0.2223 (4)
C1	−0.1481 (5)	0.5969 (4)	0.2778 (5)
C2	−0.1633 (5)	0.5828 (4)	0.3994 (5)
C3	−0.2659 (6)	0.5987 (5)	0.4228 (6)
C4	−0.3557 (6)	0.6286 (5)	0.3283 (6)
C5	−0.3433 (5)	0.6430 (5)	0.2082 (6)
C6	−0.2394 (5)	0.6279 (4)	0.1817 (5)
C7	−0.2356 (4)	0.6457 (4)	0.0543 (5)
C8	−0.1532 (4)	0.6522 (4)	−0.1198 (5)
C9	−0.0334 (4)	0.6699 (4)	−0.1234 (5)
C10	−0.0082 (5)	0.6575 (4)	−0.2511 (5)
C11	0.1647 (5)	0.6709 (4)	−0.3069 (5)
C12	0.2219 (6)	0.6607 (4)	−0.2892 (5)
C13	0.3244 (6)	0.6868 (4)	−0.3915 (6)
C14	0.4355 (6)	0.6780 (5)	−0.3848 (6)
C15	0.5061 (6)	0.6412 (5)	−0.2760 (7)
C16	0.4683 (5)	0.6143 (5)	−0.1732 (6)
C17	0.3543 (5)	0.6240 (4)	−0.1777 (5)
C18	0.2059 (5)	0.5724 (4)	0.3137 (5)
C19	0.3184 (5)	0.5641 (5)	0.3215 (5)
C20	0.3273 (5)	0.5714 (4)	0.1989 (5)

Table III. Atomic Parameters for Compound **2**

atom	x/a	y/b	z/c
Cu1	0.2307 (1)	0.3689 (2)	0.9196 (1)
Cu2	0.2916 (1)	0.3976 (2)	0.6679 (1)
O1	0.1456 (5)	0.3575 (12)	0.9830 (7)
C1	0.1360 (6)	0.3250 (13)	1.0862 (10)
C2	0.0672 (7)	0.3190 (14)	1.1115 (11)
C3	0.0545 (7)	0.2843 (14)	1.2199 (12)
C4	0.1104 (8)	0.2545 (14)	1.3073 (12)
C5	0.1771 (7)	0.2599 (12)	1.2829 (11)
C6	0.1921 (6)	0.2930 (12)	1.1740 (10)
C7	0.2645 (6)	0.2894 (12)	1.1582 (10)
N3	0.2871 (5)	0.3142 (10)	1.0623 (9)
C8	0.3637 (7)	0.2945 (13)	1.0692 (10)
C9	0.3944 (7)	0.4113 (14)	1.0011 (11)
C10	0.3813 (6)	0.3794 (13)	0.8733 (11)
O3	0.3073 (4)	0.3600 (8)	0.8316 (7)
C11	0.4246 (7)	0.2437 (15)	0.8468 (12)
C12	0.3984 (8)	0.1711 (15)	0.7354 (12)
N4	0.3752 (5)	0.2884 (11)	0.6478 (8)
C13	0.4115 (7)	0.3067 (14)	0.5674 (11)
C14	0.3942 (6)	0.4064 (14)	0.4733 (10)
C15	0.4453 (7)	0.4191 (15)	0.4004 (11)
C16	0.4325 (9)	0.5109 (16)	0.3064 (13)
C17	0.3684 (9)	0.5363 (14)	0.2832 (13)
C18	0.3174 (8)	0.5743 (14)	0.3546 (12)
C19	0.3303 (7)	0.4866 (12)	0.4546 (10)
O2	0.2818 (5)	0.4798 (9)	0.5196 (7)
N1	0.1724 (5)	0.4379 (10)	0.7818 (8)
C21	0.1020 (6)	0.4683 (12)	0.7614 (11)
C22	0.0826 (7)	0.5060 (15)	0.6470 (12)
C23	0.1449 (7)	0.4953 (14)	0.6012 (11)
N2	0.1973 (5)	0.4556 (10)	0.6818 (8)

at the Computer Center of Kyushu University. Programs used for the structure solution and anisotropic thermal parameter refinement were supplied by the local version of the UNICS system.[17] Final atomic parameters are given in Tables II and III. Tables containing structure factors, anisotropic thermal parameters, least-squares planes, and atomic deviations from these planes have been deposited as supplementary material.

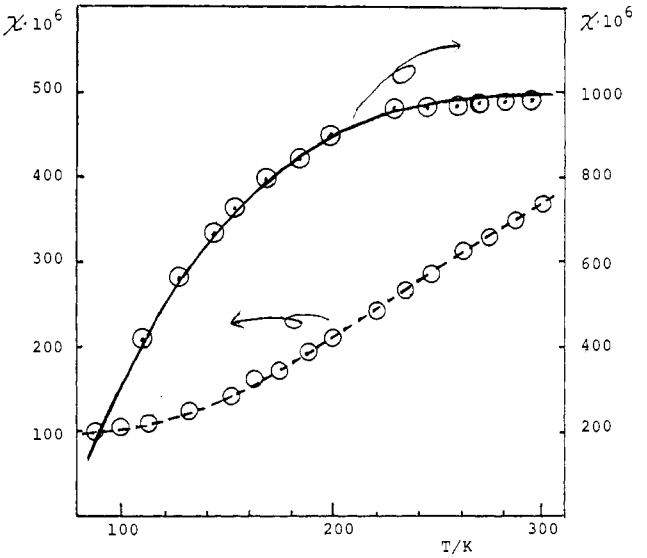

Figure 5. Magnetic susceptibilities versus temperature for **1** (⊙) and **2** (○). The solid and broken lines were calculated from the Bleaney–Bowers equation[12] by using the following parameters: (—) $2J = -310$ cm^{-1}, $g = 2.05$, $N\alpha = 30 \times 10^{-6}$ cgsemu; (---) $2J = -595$ cm^{-1} $g = 2.10$, $N\alpha = 100 \times 10^{-6}$ cgsemu.

Results and Discussion

Molecular Structures and Magnetisms of 1 and 2. The crystals of both compounds consist of discrete dinuclear molecules. The minimum intermolecular Cu–Cu distances are 4.2 and 6.1 Å, for **1** and **2**, respectively.

The ORTEP diagrams of **1** and **2** are shown in Figures 3 and 4, respectively. In both complexes two copper atoms are bridged by the alkoxide oxygen and the two nitrogens of pyrazolate ion as expected, and the whole molecule is essentially planar. There is no essential difference in molecular structures between **1** and **1**·H_2O[13] except for the difference in the planarity of bonds around the bridging oxygen; i.e., in the case of **1**·H_2O, Cu1, O3, Cu2, and C9 are coplanar, but C9 considerably deviates from the Cu1–O3–Cu2 plane in the case of **1** (cf. Table IV). As for the superexchange interaction through the alkoxide pathway, it has been claimed that the Cu–O–Cu angle is closely related to the degree of the interaction.[3-8] However, there is no significant difference in the Cu–O–Cu angles (121.7 and 121.3°) between **1** and **2**. The dihedral angle between the two coordination planes has also been regarded as a key factor to determine the spin-exchange interaction between two copper ions; i.e., the closer the angle to 180°, the larger the antiferromagnetic interaction.[18,19] On this basis, one would expect from the magnetic data a larger dihedral angle for **2** than for **1**. In practice, however, the observed angles were 172.6 and 162.6° for **1** and **2**, respectively, opposite to the expectation. The planarity of the bonds around the bridging oxygen has also been considered as the determining factor for the antiferromagnetic interaction.[13,20] In fact, there is considerable variation in the planarity of the bonds around the bridging oxygens of the complexes under consideration. However, there could not be found any systematic correlation between the planarity and the J value. For instance, in the case of **1**·H_2O the sum of the three bond angles around the bridging oxygen is 359.9°, indicating the bonds around the oxygen are practically coplanar, in spite of the fact that the $-2J$ value is the lowest among the complexes cited in Table IV; on the other hand, in the case of **1**, whose $-2J$ value

(16) *International Tables for X-Ray Crystallography*; Kynoch: Birmingham, England, 1974; Vol. IV.
(17) (a) Kawano, S. *Rep. Comput. Cent., Kyushu Univ.* **1980**, *13*, 39. (b) "Universal Crystallographic Computer Programs System (UNICS)"; Sakurai, T., Ed.; The Crystallographic Society of Japan: Tokyo, 1967.
(18) Charlot, M. F.; Jeannin, S.; Jeannin, Y.; Kahn, O.; L.-Aboul, J.; M.-Frere, J. *Inorg. Chem.* **1979**, *18*, 1675.
(19) Charlot, M. F.; Kahn, O.; Jeannin, S.; Jeannin, Y. *Inorg. Chem.* **1980**, *19*, 1411.
(20) (a) Mikuriya, M.; Toriumi, K.; Ito, T.; Kida, S. *Inorg. Chem.* **1985**, *24*, 629. (b) Nieminen, K. *Ann. Acad. Sci. Fenn., Ser. A2* **1983**, *197*, 8.

Table IV. Structural and Magnetic Parameters

	$Cu_2(L^1)(prz)$	$Cu_2(L^1)(prz)\cdot H_2O$	$Cu_2(L^2)(prz)$	$Cu_2(L^1)OCH_3(CH_3OH)$
		Distances/Å		
Cu1–Cu2	3.349	3.359	3.401	3.644
Cu1–O1	1.892	1.917	1.911	1.923
Cu1–N1	1.953	1.960	1.947	
Cu1–N3	1.945	1.929	1.940	1.920
Cu–O3	1.918	1.888	1.942	1.944
Cu2–O2	1.847	1.888	1.903	1.930
Cu2–N4	1.933	1.924	1.934	1.897
Cu2–N2	1.946	1.924	1.923	
Cu–O3	1.918	1.896	1.961	1.964
N1–N2	1.375	1.430	1.363	
		Angles/deg		
Cu1–O3–Cu2	121.7	125.1	121.3	137.7
Cu1–O3–C9	111.0	117.1		108.4
Cu1–O3–C10			126.9	
Cu2–O3–C9	110.3	117.7		107.7
Cu2–O3–C10			108.4	
O3–Cu1–N3	82.6	83.0	95.4	85.6
O3–Cu1–O1	176.4	176.3	169.2	175.9
O3–Cu1–N1	88.6	87.1	86.7	
N3–Cu1–O1	95.2	94.7	92.1	94.2
N3–Cu1–N1	163.7	169.0	175.6	
O1–Cu1–N1	94.2	95.5	86.2	
O3–Cu2–N4	82.6	83.6	91.8	86.8
O3–Cu2–O2	173.5	172.6	166.8	176.5
O3–Cu2–N2	88.4	88.0	88.0	
N4–Cu2–O2	96.2	95.3	92.8	93.9
N4–Cu2–N2	166.2	170.0	164.9	
O2–Cu–N2	93.8	93.7	90.8	
Cu1–N1–N2	120.0	119.4	122.8	
Cu2–N2–N1	120.6	120.2	120.6	
angle between two coordn planes	172.6	176.2	162.8	164.7
sum of angles around O3	343.0	359.9	356.6	353.8
		$-2J/cm^{-1}$		
	310	240	595	635

is the second lowest, the deviation from the plane is the largest, as seen in Table IV. Therefore, this factor also does not seem to be the main factor for the difference in J values between **1** and **2**. Thus, all the criterions so far widely accepted on the magnetism of planar binuclear copper complexes have failed to account for the experimental results. Accordingly, we have examined the orbitals contributing to the superexchange interaction in more detail.

Orbitals Contributing to Superexchange Interaction. The copper 3d orbitals possessing unpaired electrons (denoted as d_1 and d_2 hereafter), $2p_x$, $2p_y$, and 2s orbitals of bridging oxygen, and HOMOs on the pyrazolate nitrogens should contribute effectively to the superexchange interaction in the present system.

A question may arise at this stage as to whether the superexchange through the pyrazolate bridge is strong enough to affect the $-2J$ value of 200–300 cm^{-1}. It is difficult to give a definite answer to this question at present, since in our knowledge no magnetic datum is available for purely pyrazolate-bridged dicopper complexes. However, triazolate-bridged dicopper(II) complexes were reported to show fairly strong antiferromagnetic interaction ($-2J$ = 204–236 cm^{-1}).[21] Therefore, in analogy with this fact the pyrazolate bridge may induce a fairly strong antiferromagnetism in the present complexes. In addition to this, one should notice that the J value of a doubly heterobridged system like the present complexes is not a simple algebraic sum of J values of the component singly bridged systems (cf. eq 5); thereby, the presence of a pyrazolate bridge may affect the J value considerably even if its antiferromagnetic interaction is much weaker than that of alkoxide bridge. More detailed discussion is made in the later part of this paper.

Molecular orbitals of the pyrazolate ion were calculated by the CNDO/2 method.[22,23] The HOMOs that interact with the copper

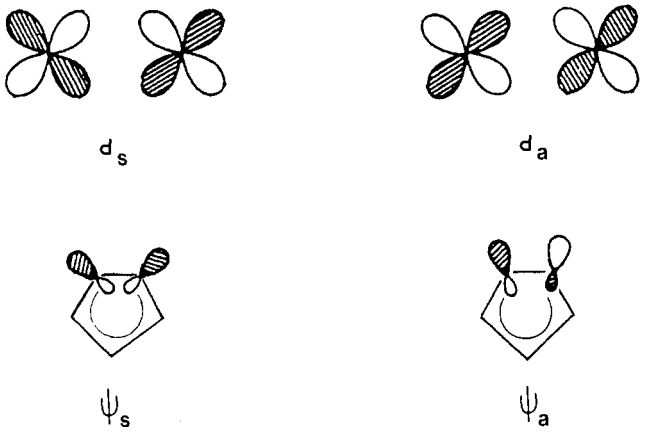

Figure 6. Phase and spacial distribution of orbitals contributing to the superexchange interaction through the pyrazolate bridge.

d orbitals are denoted as ψ_s and ψ_a and expressed in terms of LCAOs as in (1) and (3), where the subscripts s and a refer to

$$\psi_s = 0.114[s(N1) + s(N2)] + 0.489[p_x(N1) - p_x(N2)] + 0.326[p_y(N1) + p_y(N2)] + (\text{terms of carbon orbitals}) \quad (1)$$

$$\epsilon(\psi_s) = -5.07 \text{ eV} \quad (2)$$

$$\psi_a = 0.287[s(N1) - s(N2)] + 0.098[p_x(N1) + p_x(N2)] + 0.546[p_y(N1) - p_y(N2)] + (\text{terms of carbon orbitals}) \quad (3)$$

$$\epsilon(\psi_a) = -5.24 \text{ eV} \quad (4)$$

"symmetric" and "antisymmetric", respectively, with respect to the symmetry plane perpendicular to the N–N bond. The pa-

(21) Prins, R.; Birker, P. J. M. W. L.; Haasnoot, J. G.; Verschoor, G. C.; Reedijk, J. *Inorg. Chem.* **1985**, *24*, 4128.
(22) Pople, J. A.; Segal, G. A. *J. Chem. Phys.* **1966**, *44*, 3289.
(23) The calculation was performed by a microcomputer with the program kindly supplied by Dr. Tominaga of Adeka Argus Chemical Co. Ltd.: Tominaga, N. *Kagaku no Ryoiki* **1982**, *36*, 724.

Table V. Classification of Orbitals in Terms of Irreducible Representations of the C_{2v} Point Group

	Cu1, Cu2	O3	N1, N2
a_1	d_s[a]	p_y	ψ_s
b_2	d_a[a]	p_x	ψ_a

[a] $d_s = d_1 - d_2$; $d_a = d_1 + d_2$ (cf. Figure 5).

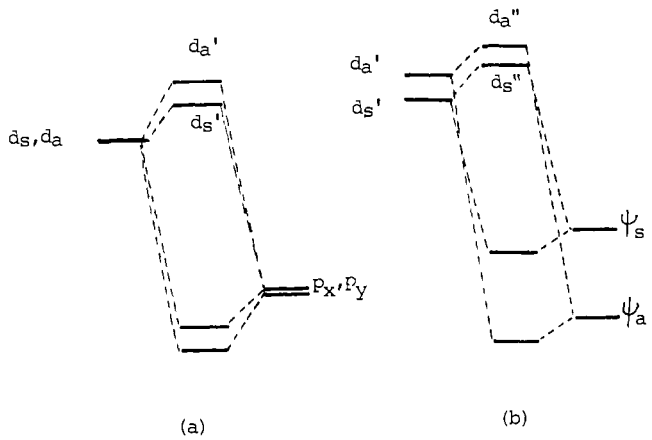

Figure 7. Qualitative orbital energy diagrams showing the interaction between the magnetic orbitals and bridging-group orbitals: (a) single-alkoxide-bridged system; (b) further interaction due to the addition of a pyrazolate bridge to (a).

rameters used for the calculations are listed in the Appendix. The phase and spacial distribution of these orbitals are qualitatively illustrated in Figure 6.

The symmetry of the complexes **1** and **2** is represented by C_{2v}, under which the orbitals are classified into irreducible representations according to their transformation properties, as shown in Table V.

Orbital Energies of 3: A Single-Alkoxide-Bridged Complex. Table V indicates that the a_1 and b_2 molecular orbitals are formed from d_s and p_y and from d_a and p_x, respectively, to form the Cu–O–Cu bond. Since the Cu–O–Cu angle (121–138°) is much larger than 90°, $S(d_a,p_x)$ should be substantially larger than $S(d_s,p_y)$, where $S(\phi_i,\phi_j)$ represents the overlap integral between ϕ_i and ϕ_j. Hence, d_a and d_s split as illustrated in Figure 7a, and the molecular orbitals thus formed are denoted as d_a' and d_s', respectively. Consequently, the complex shows a strong antiferromagnetism ($2J = -635$ cm^{-1}).[10]

Orbital Energies of a Complex Possessing Alkoxide and Pyrazolate Bridges As in the Cases of 1, 1·H$_2$O, and 2. According to the orbital symmetries, d_a' and d_s' further interact with ψ_a and ψ_s, respectively, forming new molecular orbitals d_a'' and d_s'' (cf. Figure 7b). The energy gap between these two orbitals should be the determining factor for the J value, since according to Hoffmann[5]

$$-2J = \frac{[\epsilon(d_a'') - \epsilon(d_s'')]^2}{J_{11} - J_{12}} - 2K_{12} \qquad (5)$$

where J_{11}, J_{12}, and K_{12} are the conventional interelectronic repulsion integrals of magnetic orbitals localizing in Cu1 and Cu2. In cases where the bridging structures are all similar and $-2J$ is some hundred reciprocal centimeters, as in the present complexes, J_{11}, J_{12}, and K_{12} may be regarded as nearly constant; hence, the variation of J values among the present complexes should be mostly due to the variation of $\epsilon(d_a'') - \epsilon(d_s'')$. It should be noted that $-2J$ is linear not versus $\epsilon(d_a'') - \epsilon(d_s'')$ but versus the square of $\epsilon(d_a'') - \epsilon(d_s'')$, according to eq 5, and that $\epsilon(d_a'')$ and $\epsilon(d_s'')$ are nearly linear to the square of the overlap integrals, $S(d_a'',\psi_a)$ and $S(d_s'',\psi_s)$, respectively.[24] Therefore, even a small change in $\epsilon(d_a'')$ or $\epsilon(d_s'')$ caused by the various factors may bring about a remarkable change in the J value.

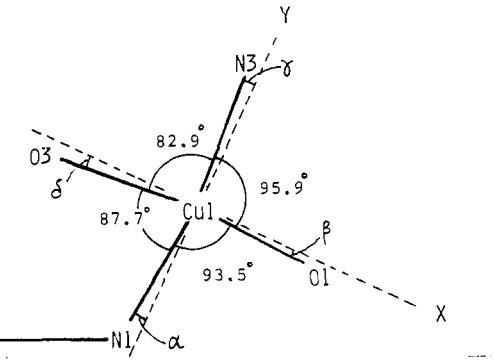

Figure 8. Projection of Cu1 and the donor atoms onto the best plane formed by these atoms. (The broken lines are the axes of the magnetic d orbital.)

The energies of d_a'' and d_s'' depend on two factors, i.e., (i) the energy differences between the interacting orbitals, $\epsilon(d_a)$ and $\epsilon(\psi_a)$, and $\epsilon(d_s)$ and $\epsilon(\psi_s)$, and (ii) the overlap integrals, $S(d_a,\psi_a)$ and $S(d_s,\psi_s)$. Since the orbital energy of ψ_s is higher than that of ψ_a by 0.17 eV (1370 cm^{-1}) (cf. (2) and (4)), which must be substantially larger than the energy gap between d_a' and d_s', factor (i) of the above discussion should be increasing for the energy gap of d_a'' and d_s'', hence working complementarily with the alkoxide bridge to enhance antiferromagnetic interaction. We will call a change that causes an increase in the energy gap a complementary factor and, vice versa, a change that causes a decrease in the gap a countercomplementary factor.

In the following discussion, we will focus our attention on the effect that the change in orientation of the local magnetic d orbitals has upon this energy gap. The change in orientation is caused by the change in chelate ring size (5 or 6) upon the replacement of ligand L^1 by ligand L^2.

The overlap integrals can be expressed as

$$S(d_s,\psi_s) = 0.161(\cos(2\alpha))S(3d,2s) + 0.745(\cos(2\alpha))S(3d_\sigma,2p_\sigma) + 0.368(\sin(2\alpha))S(3d_\pi,2p_\pi) \qquad (6)$$

$$S(d_a,\psi_a) = 0.406(\cos(2\alpha))S(3d,2s) + 0.738(\cos(2\alpha))S(3d_\sigma,2p_\sigma) - 0.266(\sin(2\alpha))S(3d_\pi,2p_\pi) \qquad (7)$$

where α is the angle between the Cu–N bond and an axis of the magnetic d orbital whose orientation is chosen so as to best extend its lobes toward the donor atoms (cf. Figure 8): the rigorous definition and the process of the calculation are cited in the Appendix. The difference between $S(d_a,\psi_a)$ and $S(d_s,\psi_s)$ is an important factor to expand or contract the energy separation of d_s'' and d_a'' and is denoted as $S(a-s)$. From (6) and (7)

$$S(a-s) = S(d_a,\psi_a) - S(d_s,\psi_s) = 0.245S(3d,2s)\cos(2\alpha) - 0.007S(3d_\sigma,2p_\sigma)\cos(2\alpha) - 0.634S(3d_\pi,2p_\pi)\sin(2\alpha) \qquad (8)$$

In the case of **1**, $\alpha = 3.6°$; hence

$$S(a-s)(1) = 0.243S(3d,2s) - 0.007S(3d_\sigma,2p_\sigma) - 0.082S(3d_\pi,2p_\pi) \qquad (9)$$

In the case of **2**, $\alpha = -0.6°$; hence

$$S(a-s)(2) = 0.245S(3d,2s) - 0.007S(3d_\sigma,2p_\sigma) + 0.013S(3d_\pi,2p_\pi) \qquad (10)$$

Rough values of the overlap integrals for the present complexes can be estimated from the tables of Jaffe et al.[25] and Kuroda and Ito;[26] $S(3d_\sigma,2p_\sigma) \approx 0.06$, $S(3d,2s) \approx 0.04$, and $S(3d_\pi,2p_\pi) \approx 0.02$. Considering these values with (8) and (9), one can conclude that $S(a-s)$ is definitely larger than zero in both cases; i.e.

$$S(d_a,\psi_a) > S(d_s,\psi_s) \qquad (11)$$

Accordingly, it is clear that factor ii in the above discussion tends

(24) Jørgensen, C. K.; Papalardo, R.; Schmidtke, H. H. *J. Chem. Phys.* **1963**, *39*, 1422.

(25) (a) Jaffe, H. H.; Doal, G. O. *J. Chem. Phys.* **1953**, *21*, 196. (b) Jaffe, H. H. *Ibid.* **1953**, *21*, 258.

(26) Kuroda, Y.; Ito, K. *Nippon Kagaku Zasshi* **1955**, *76*, 545.

to reduce the energy separation between d_a'' and d_s''. This is the trend opposite to factor i.

It is difficult to estimate from this rough calculation which factor is superiorly operating in the present complexes. However, the experimental results have shown that the $2J$ value of **2** (-595 cm^{-1}) is very close to that of **3** (-635 cm^{-1}), indicating that both effects are almost counterbalanced in **2**.

From (9) and (10)

$$S(a\text{-}s)(\mathbf{1}) - S(a\text{-}s)(\mathbf{2}) = -0.002S(3d,2s) - 0.095S(3d_\pi,2p_\pi) < 0$$

$$\therefore S(a\text{-}s)(\mathbf{1}) < S(a\text{-}s)(\mathbf{2}) \quad (12)$$

This clearly indicates that the effect of factor ii for **1** is weak compared with that for **2**. As the result, the energy separation of d_a'' and d_s'' for **1** is reduced in some degree compared with that for **2**; in other words, in the case of **1** the pyrazolate bridge exerts a countercomplementary effect on the antiferromagnetic interaction caused by the alkoxide bridge. This effect may be ascribed as the main factor for the smaller $-2J$ value of **1** compared with that of **2**, though a definite conclusion cannot be drawn with this qualitative discussion.

Conclusion

In alkoxide-bridged dicopper(II) complexes antiferromagnetic interaction through the alkoxide oxygen is large when the Cu–O–Cu angle is large, as demonstrated in the case of **3**. When two copper(II) ions are doubly bridged with alkoxide oxygen and pyrazolate nitrogens, as in the cases of **1** and **2**, the effect of the pyrazolate bridge is to increase or decrease the energy separation between $\epsilon(d_a'')$ and $\epsilon(d_s'')$, depending on the relative degree of interaction between d_a and ψ_a and between d_s and ψ_s. The strong interaction of the former combination promotes the complementary effect, and of the latter, the countercomplementary effect. In the case of **2**, judging from the experimentally obtained $2J$ value, the effects of these two factors seem to be counterbalanced and affect very little the antiferromagnetism caused by the alkoxide bridge. However, in going from **2** to **1**, the magnetic d orbitals are slightly rotated with the change of the six-membered chelate ring into the five-membered ring, bringing about the increase of $S(d_s,\psi_s)$ and the decrease of $S(d_a,\psi_a)$. As a result, the pyrazolate bridge tends to compensate for the antiferromagnetism effected by the alkoxide bridge in **1**. Thus, this is in line with the experimental fact that the $-2J$ value of **1** is much smaller than that of **2**.

Appendix

Determination of the Orientation of the Magnetic d Orbital. The orientation of the magnetic d orbital was determined so as to attain maximum overlapping with the four σ-donor orbitals. Figure 8 shows the projection of Cu1 and the donor atoms onto the coordination plane together with the axes of the magnetic d orbital (broken lines). The angles formed by the coordination bonds and the axes of the d orbital are denoted as α, β, γ, and δ, as depicted in Figure 8. In order to fulfill the requirement of maximum overlapping, the following function was minimized:

$$F(\alpha) = \alpha^2 + \beta^2 + \gamma^2 + \delta^2 = \alpha^2 + (\alpha + 90 - 93.5)^2 + (\alpha + 180 - 93.5 - 95.9)^2 + (\alpha + 270 - 93.5 - 95.9 - 82.4)^2 = 4\alpha^2 - 29.4\alpha + 103.9 \quad (13)$$

If $dF(\alpha)/d\alpha = 0$, then $\alpha = 3.7°$. The same value was obtained for the α about the coordination plane of Cu2.

Table VI. Parameters Used for the CNDO/2 Calculation[a]

	H	C	N
μ by Slater	1.20	1.625	1.95
$(I_s + A_s)/2$	7.176	14.051	19.316
$(I_p + A_p)/2$		5.572	7.275
β	−9	−21	−25
z	1	4	5

	atomic coordinates/Å		
atom[b]	x	y	z
N1	−0.7000	0.0000	0.0000
N2	0.7000	0.0000	0.0000
C3	1.0583	1.2496	0.0000
C4	0.0000	2.0501	0.0000
C5	−1.0583	1.2496	0.0000
H6	2.0911	1.5654	0.0000
H7	0.0000	3.1301	0.0000
H8	−2.0911	1.5654	0.0000

[a] I_s and A_s represent the ionization energy and electron affinity for s orbitals (1s for H; 2s for C and N) in electronvolts. β is the parameter for each atom in the relation $H_{rs} = S_{rs}(\beta_A + \beta_B)/2$. [b] Labeling diagram:

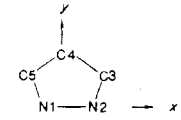

In a similar way, $\alpha = -0.6°$ in the case of **2**.

Overlap Integrals between d_s and ψ_s and between d_a and ψ_a. When the x and y axes in Figure 8 are rotated clockwise by α, the d_1 orbital, which was defined by the x and y axes as $d_{x^2-y^2}$, is expressed in terms of the new coordinate system as

$$d_1 = (\cos(2\alpha))d_{x^2-y^2} + (\sin(2\alpha))d_{xy} \quad (14)$$

The ψ_s and ψ_a orbitals can be expressed as the sum of the orbitals on N1, N2, and the neighboring carbon atoms:

$$\psi_s = \phi_{s1} + \phi_{s2} + \phi_{sC} \quad (15)$$

$$\psi_a = \phi_{a1} + \phi_{a2} + \phi_{aC} \quad (16)$$

These orbitals can be described in terms of the new coordinate system in which the y axis is on the Cu1–N1 bond:

$$\phi_{s1} = 0.114s + 0.489((\cos 30°)p_x + (\sin 30°)p_y) + 0.326(-(\cos 60°)p_x + (\sin 60°)p_y) = 0.114s + 0.260p_x + 0.527p_y \quad (17)$$

From (14) and (17)

$$S(d_1,\phi_{s,1}) = 0.114(\cos(2\alpha))S(3d,2s) + 0.527(\cos(2\alpha))S(3d_\sigma,2p_\sigma) + 0.260(\sin(2\alpha))S(3d_\pi,2p_\pi)$$

Since $d_s = (d_1 - d_2)/2^{1/2}$ and $S(d_2,\phi_{s2}) = -S(d_1,\phi_{s1})$

$$S(d_s,\psi_s) = 2S(d_1,\phi_{s1})/2^{1/2} = 0.161(\cos(2\alpha))S(3d,2s) + 0.745(\cos(2\alpha))S(3d_\sigma,2p_\sigma) + 0.368(\sin(2\alpha))S(3d_\pi,2p_\pi) \quad (6)$$

Equation 7 was also obtained by the same principle.

Supplementary Material Available: Tables of bond distances and angles, anisotropic thermal parameters, least-squares planes, and atomic deviations from these planes (8 pages); tables of structure factors (15 pages). Ordering information is given on any current masthead page.